Laboratory Investigation (2010) 90, 414–425

Promoter hypermethylation of *FBXO32*, a novel TGF-β/SMAD4 target gene and tumor suppressor, is associated with poor prognosis in human ovarian cancer

Jian-Liang Chou[1,2], Her-Young Su[3], Lin-Yu Chen[1,2], Yu-Ping Liao[4], Corinna Hartman-Frey[5], Yi-Hui Lai[1,2], Hui-Wen Yang[1,2], Daniel E Deatherage[6], Chieh-Ti Kuo[6], Yi-Wen Huang[6], Pearlly S Yan[6], Shu-Huei Hsiao[1,7], Chien-Kuo Tai[1,2], Huey-Jen L Lin[6,8], Ramana V Davuluri[9], Tai-Kuang Chao[10], Kenneth P Nephew[5], Tim H-M Huang[6], Hung-Cheng Lai*[,3,11] and Michael W-Y Chan*[,1,7]

Resistance to TGF-β is frequently observed in ovarian cancer, and disrupted TGF-β/SMAD4 signaling results in the aberrant expression of downstream target genes in the disease. Our previous study showed that *ADAM19*, a SMAD4 target gene, is downregulated through epigenetic mechanisms in ovarian cancer with aberrant TGF-β/SMAD4 signaling. In this study, we investigated the mechanism of downregulation of *FBXO32*, another SMAD4 target gene, and the clinical significance of the loss of *FBXO32* expression in ovarian cancer. Expression of *FBXO32* was observed in the normal ovarian surface epithelium, but not in ovarian cancer cell lines. *FBXO32* methylation was observed in ovarian cancer cell lines displaying constitutive TGF-β/SMAD4 signaling, and epigenetic drug treatment restored *FBXO32* expression in ovarian cancer cell lines regardless of *FBXO32* methylation status, suggesting that epigenetic regulation of this gene in ovarian cancer may be a common event. In advanced-stage ovarian tumors, a significant (29.3%; $P<0.05$) methylation frequency of *FBXO32* was observed and the association between *FBXO32* methylation and shorter progression-free survival was significant, as determined by both Kaplan–Meier analysis ($P<0.05$) and multivariate Cox regression analysis (hazard ratio: 1.003, $P<0.05$). Reexpression of *FBXO32* markedly reduced proliferation of a platinum-resistant ovarian cancer cell line both *in vitro* and *in vivo*, due to increased apoptosis of the cells, and resensitized ovarian cancer cells to cisplatin. In conclusion, the novel tumor suppressor *FBXO32* is epigenetically silenced in ovarian cancer cell lines with disrupted TGF-β/SMAD4 signaling, and *FBXO32* methylation status predicts survival in patients with ovarian cancer.
Laboratory Investigation (2010) **90,** 414–425; doi:10.1038/labinvest.2009.138; published online 11 January 2010

KEYWORDS: ovarian cancer; epigenetics; TGF-β; FBXO32

Ovarian cancer is the fifth leading cause of death in women and the most deadly of gynecological malignancies.[1] The lifetime risk of ovarian cancer in women is $\sim$1.5%.[2] As ovarian cancer has few symptoms early in its course, the majority of patients are diagnosed with advanced-stage disease. Despite advances in chemotherapy, the poor prognosis for patients with ovarian cancer is reflected in the $<$20% 5-year survival rate after initial diagnosis for patients with stage III and IV disease, whereas survival of patients with stage I or II disease is $>$80% for the same period.[3] Current

[1]Department of Life Science, National Chung Cheng University, Min-Hsiung, Chia-Yi, Taiwan, ROC; [2]Institute of Molecular Biology, National Chung Cheng University, Min-Hsiung, Chia-Yi, Taiwan, ROC; [3]Graduate Institute of Medical Sciences, National Defense Medical Center, Taipei, Taiwan, ROC; [4]Graduate Institute of Life Sciences, National Defense Medical Center, Taipei, Taiwan, ROC; [5]Department of Medical Sciences, Indiana University School of Medicine, Bloomington, IN, USA; [6]Department of Molecular Virology, Immunology, and Medical Genetics, Human Cancer Genetics Program, Comprehensive Cancer Center, the Ohio State University, Columbus, OH, USA; [7]Human Epigenomics Center, National Chung Cheng University, Min-Hsiung, Chia-Yi, Taiwan, ROC; [8]Divison of Medical Technology, School of Allied Medical Professions, the Ohio State University, Columbus, OH, USA; [9]Center for Systems and Computational Biology, Molecular and Cellular Oncogenesis Program, The Wistar Institute, Philadelphia, PA, USA; [10]Department of Pathology, Tri-Service General Hospital, National Defense Medical Center, Taipei, Taiwan, ROC and [11]Department of Obstetrics and Gynecology, National Defense Medical Center, Taipei, Taiwan, ROC

*Correspondence: Dr MWY Chan, PhD, Room 452, Department of Life Science and Human Epigenomics Center, 168 University Road, National Chung Cheng University, Min-Hsiung, Chia-Yi, 621, Taiwan, ROC.
E-mail: biowyc@ccu.edu.tw or
Dr H-C Lai, MD, PhD, Department of Obstetrics and Gynecology, Tri-Service General Hospital, National Defense Medical Center, 5F, 325, Sec 2, Cheng-Gong Rd., Neihu District, Taipei 114, Taiwan, ROC.
E-mail: hclai@ndmctsgh.edu.tw

Received 30 April 2009; revised 3 November 2009; accepted 23 November 2009

prognostic indicators using clinicopathological variables, including stage and grade, neither accurately predict clinical outcomes nor provide biological insight into the disease. Thus, a better understanding of the molecular carcinogenesis of ovarian cancer is required for developing more reliable prognostic markers.

The transforming growth factor-β signaling pathway has an important role in controlling proliferation, differentiation, and other cellular processes, including the growth of ovarian surface epithelial (OSE) cells.[4] With each ovulation, the OSE covering the ovary undergoes rupture, followed by proliferation-mediated repair.[5] The growth inhibitory effect of TGF-β on the OSE may have a key role in preventing overproliferation of OSE,[5] and dysregulation of TGF-β signaling may be crucial to the development of epithelial ovarian cancer. In addition, resistance to TGF-β signaling is commonly observed in ovarian cancer,[6,7] suggesting that diminished responsiveness to TGF-β is a key event. However, few studies have examined the consequences of disrupted TGF-β signaling in ovarian cancer.

Ovarian tumorigenesis is a multistep process that includes the accumulation of acquired (somatic) epigenetic changes in critical genes.[8] Epigenetic alterations, including DNA methylation and histone modifications, have important roles in gene regulation,[9–11] and we along with others[12–16] have previously shown that tumor-suppressor genes can be transcriptionally silenced by epigenetic modifications in ovarian cancer. We have also shown that epigenetically modified genes can be used for both ovarian cancer diagnosis and prognosis.[17,18]

Our previous study using chromatin immunoprecipitation microarray (ChIP–Chip) identified *FBXO32* as a TGF-β/SMAD target gene in OSE.[19] FBXO32 (also known as atrogin-1) is a member of the F-box protein family and constitutes one of the four subunits of the ubiquitin protein ligase complex.[20,21] The FBXO32 protein has been reported to have a role in muscle atrophy,[22] and recent findings suggest that FBXO32 is a novel apoptosis regulator[23] and is negatively regulated by a pro-survival signal.[24] Interestingly, Tan *et al*[23] also showed that *FBXO32* was transcriptionally silenced by epigenetic mechanisms in MCF-7 breast cancer cells. In this study, we found that *FBXO32* was downregulated in a panel of ovarian cancer cell lines. Promoter hypermethylation of *FBXO32* was observed in ovarian cancer cells, showing constitutive SMAD4 nuclear translocation.[15] Restoration of *FBXO32* suppressed ovarian cancer cell growth *in vitro* and xenografts *in vivo*; this suppression was due to increased apoptosis. *FBXO32* resensitized drug-resistant ovarian cancer cells to cisplatin. Importantly, ovarian cancer patients with high *FBXO32* methylation had significantly shorter progression-free survival (PFS) than patients with no or low methylation. These results suggest that dysregulation of TGF-β/SMAD4 signaling may lead to aberrant DNA methylation of *FBXO32* in ovarian cancer. *FBXO32* may be a novel tumor suppressor, and the methylation status of *FBXO32* may predict survival in ovarian cancer.

MATERIALS AND METHODS

Patient Samples

A total of 96 ovarian cancer samples were obtained from the Tri-Service General Hospital (Taipei, Taiwan) (Supplementary Table S1). Five normal OSE (NOSE) cells were acquired from patients during surgery for benign gynecological disease at the Indiana University as described previously.[17,25] All studies involving human ovarian epithelial samples were approved by the Institutional Review Boards of the Tri-Service General Hospital (Taiwan) and the Indiana University.

Cell Culture and Epigenetic Treatment

Immortalized OSE (IOSE) cells were derived by transducing the catalytic subunit of human telomerase and the papilloma virus subunit E7 into primary ovarian epithelial cells, as described previously.[26] Cells were maintained in a 1:1 mixture of medium 199 (Sigma, St Louis, MO, USA) and 105 (Sigma) supplemented with 10% fetal bovine serum (FBS) (Invitrogen, Carlsbad, CA, USA), 400 ng/ml hydrocortisone (Sigma), 10 ng/ml EGF, and 50 Units/ml of penicillin/streptomycin (Invitrogen).[26] Ovarian cancer cell lines, namely A2780, CP70, MCP2, MCP3, were propagated with RPMI 1640 (Invitrogen) containing 10% FBS. The HeyC2 cell was cultured with DMEM containing 5% FBS, 1% NEAA, 1% Gln, and 1% HEPES. The SKOV3 cell was cultured with McCoy's 5A containing 10% FBS, 1% NEAA, 1% Gln, and 1% HEPES. For epigenetic treatment, 1×10^6 cells were seeded onto 90-mm plates and treated with 5 μM 5′-aza-2′-deoxycytidine (5-azaDC; Sigma) for 72 h or with trichostatin A (TSA, 0.5 μM; Sigma) for 12 h. For 5-azaDC treatment, media were changed and a new drug was added every 24 h.

DNA Extraction

DNA was extracted using the Tissue and Cell Genomic DNA Purification Kit (Genemark, Taiwan). DNA was eluted in 50 μl distilled water and stored at -20°C until use.

Bisulfite Conversion and Combined Bisulfite Restriction Analysis

Genomic DNA (0.5 μg) was bisulfite modified using the EZ DNA Methylation Kit (Zymo Research, Orange, CA, USA) according to the manufacturer's protocol. For combined bisulfite restriction analysis (COBRA), bisulfite-modified DNA was first amplified using *FBXO32*-specific primer, followed by digestion with 20 Units of AciI (GGCG) or Hinp1I (GCGC) (New England Biolabs, Ipswich, MA, USA). *FBXO32*-specific primers were: forward primer, 5′ ATTGG TTAGTGATAGTTAAGGGGT and reverse primer, 5′ GGGAT AACGGTGTTTTGG (369 bp). After bisulfite conversion of methylated original genomic sequence, multiple sites for each of these enzymes were present; however, no sites were present in the bisulfite-converted original unmethylated genomic sequence. The digested PCR products were separated by gel electrophoresis using 3% GenePure high-resolution agarose

(ISC BioExpress, Kaysville, UT, USA) and stained with ethidium bromide.

Methylation-Specific PCR and Real-Time Quantitative Methylation-Specific PCR

The bisulfite-modified DNA was subjected to methylation-specific PCR (MSP) and real-time quantitative MSP (qMSP) as described previously.[27] Primers targeting the promoter region of *FBXO32* were as follows: forward, 5′TTAGTTTT GCGGACGGTTC and reverse, 5′ CGGGGCGTATTTTTTT AAGC (187 bp). For qMSP, β-actin (*ACTB*) or collagen (*COL2A1*) were used to normalize for the input DNA. A region devoid of any CpG dinucleotide was amplified using the following primer sequences: for *ACTB*, forward primer 5′ TGGTGATGGAGGAGGTTTAGTAAGT and reverse primer 5′ AACCAATAAAACCTACTCCTCCCTTAA (133 bp); for *COL2A1*, forward primer 5′ TCTAACAATTATAAACTCCAA CCACCAA and reverse primer 3′ GGGAAGATGGGATAGA AGGGAATAT. The amount of methylated *FBXO32*, *ACTB*, and *COL2A1* were determined by the threshold cycle number (C_t) for each sample against a standard curve generated by SssI-treated DNA-MSP cloned fragment. The percentage of *FBXO32* methylation was calculated as the FBXO32:ACTB or FBXO32:COL2A1 ratio of a sample divided by the same ratio of SssI-treated sperm DNA (Millipore, Billerica, MA, USA) and multiplied by 100.

RNA Extraction and Quantitative Reverse Transcription-PCR

Total RNA from cell lines was extracted using Trizol (Invitrogen) as described previously.[28] In brief, 1 μg of total RNA was treated with DNase I (amplification grade, Invitrogen) before first-strand cDNA synthesis using reverse transcriptase (Superscript II RT, Invitrogen). PCR reactions were carried out using ABI 7500 real-time PCR system (Applied Biosystems, Foster city, CA, USA). *FBXO32* and *GAPDH* cDNA were amplified with the following primer sequences: *FBXO32* forward, 5′AAGTCTGTGCTGGTCGGG AA and reverse, 5′AGTGAAGGTGAGGCCTTTGAAG; *GAPDH* forward, 5′ CCCCTTCATTGACCTCAACTACAT and reverse, 5′TCACCATCTTCCAGGAGCG. The relative expression of *FBXO32* was calculated using comparative C_t method.

Plasmid Construction and Colony-Formation Assay

The full-length human *FBXO32* cDNA was cloned from IOSE cells. The fragment was inserted into the XhoI–BamHII sites of vector pIRES_EGFP (Promega, Madison, WI, USA) or pcDNA3.1 (Invitrogen). Plasmid constructs were verified by sequencing. Approximately 1.5 μg of *FBXO32* expression vector or empty vector was transfected into CP70 or HeyC2 cells using Transfectam Reagent (Promega) according to the manufacturer's protocol. Twenty-four hours after transfection, cells were replated in triplicate and cultured for 3 weeks in RPMI 1640 containing 10% FBS supplemented with 400 μg/ml G418 (Invitrogen, Paisley, UK). The surviving colonies were stained with 0.4% crystal violet (Sigma) in 50% methanol, and visible colonies were counted. Experiments were repeated twice and the average number of colonies from six plates for each plasmid was obtained.

Cell Proliferation Assay

Cell growth was assessed by counting cell numbers or by MTS assay, as described previously.[15] In brief, for cell number counts, 5×10^4 cells were seeded onto a 35-mm plate, and cell numbers were determined daily using a hemacytometer. For MTS assays, $\sim$1000 cells were seeded in 96-well plates for 4 days with or without various concentrations of cisplatin (Sigma). Cell growth was determined using the CellTiter 96 Aqueous One Solution Cell Proliferation Assay Kit (Promega), according to the manufacture's protocol. Relative cell numbers were assessed using a 96-well ELISA plate reader with an absorbance set at 490 nM.

Flow Cytometry Analysis

Cells were cultured with or without cisplatin (1 μg/ml) for 24 h, collected after brief trypsinization, washed with PBS, and fixed in 70% ethanol for 24 h at -20°C. Cells were then treated with 0.1 mg/ml RNase, stained with 10 μg/ml propidium iodide (Sigma) at 37°C for 30 min and analyzed using FACScan flow cytometer (Becton Dickinson, Franklin Lakes, NJ, USA). The percentage of apoptotic cells in the sub-G1 area was analyzed using the software cell quest (Becton Dickinson). The cell-cycle distribution was quantified using the ModFit LT software (Becton Dickinson).

In vivo Tumorigenicity Assay

A total of four, 8-week-old, athymic nude mice (BALB/cByJNarl) were obtained from the National Laboratory Animal Center (Taiwan). All mice were kept under specific pathogen-free conditions using a laminar airflow rack with free access to sterilized food and autoclaved water. All experiments were conducted after obtaining license from the Animal Experimentation Ethics Committee of the National Chung Cheng University. Overall, 1×10^5 cells of CP70 stably transfected with pcDNA3.1/FBXO32 or empty vector were resuspended in a mixture of 0.1 ml of medium and Matrigel (1:1) (BD Bioscience, San Jose, CA, USA). Cell suspension was then injected subcutaneously into the flank of each mouse (day 0). Tumor size was measured daily with calipers in length (L) and width (W). Tumor volume was calculated using the formula ($L \times W^2/2$). At the end of experiment, all mice were killed by cervical dislocation.

Immunohistochemistry

Paraffin-embedded tissues of the above-mentioned patient samples were retrieved from the Department of Pathology (Tri-Service General Hospitals, Taiwan). Tissue sections were dewaxed in xylene, rehydrated in alcohol, and immersed in 3% hydrogen peroxide for 10 min to suppress endogenous

peroxidase activity. Antigen retrieval was performed by heating each section at 100°C for 30 min in 0.01 mol/l sodium citrate buffer (pH 6.0). After 5-min rinses three times in phosphate-buffered saline (PBS), sections were incubated for 1 h at room temperature with a mouse polyclonal anti-FBX32 antibody (ab67866, Abcam, Cambridge, UK) diluted 1:100 in PBS, and bound antibodies were detected with a streptavidin–biotin–peroxidase system (Dako, Glostrup, Denmark) and 3,3′-diaminobenzidine substrate-chromogen solution (Dako). Slides were counterstained with hematoxylin and examined by an experienced pathologist (T-K Chao).

Statistical Analysis

Multivariate survival analysis was determined using Cox proportional hazards model with the DNA methylation level as a continuous variable. The multivariate Cox proportional hazards model was used to determine the independent prognostic value of DNA methylation level, stage, and age. PFS) and overall survival (OS) were assessed by Kaplan–Meier analysis using log-rank test. PFS was defined as the duration from the day of diagnosis or chemotherapy to detection of new lesions or progression of residual lesions. OS was defined as the duration from the day of diagnosis to death. A DNA methylation level at 30% (level of methylation in OSE cells) was used as a cutoff. It is also noted that there were 37 patients with low methylation level ($<15\%$) and low OS (<36 months). This extreme group of patients was excluded from some analysis as specified (Supplementary Figure S4). Fisher's exact test or the Mann–Whitney *U* test was also used to compare parameters of different groups. All statistical calculations were carried out using statistical package SPSS version 13.0 for windows (SPSS, Chicago, IL, USA). $P<0.05$ was considered significant.

RESULTS

FBXO32 Expression Correlates with Promoter Methylation in Ovarian Cancer Cell Lines

On the basis of our recent ChIP–Chip experiment identifying *FBXO32* as a candidate TGF-β/SMAD4 target in IOSE (Supplementary Figure S1),[19] it was of interest to examine the expression of *FBXO32* in a panel of ovarian cancer cell lines (namely HeyC2, SKOV3, MCP3, MCP2, A2780, and CP70). Low or no expression of *FBXO32* mRNA was observed in all ovarian cancer cell lines as compared with IOSE cells (Figure 1). As a previous study showed that downregulation of *FBXO32* correlated with promoter hypermethylation in breast cancer MCF-7 cells,[23] we examined whether *FBXO32* was silenced by a similar mechanism in ovarian cancer. COBRA was first conducted to determine the methylation status of a 400-bp region of the promoter. Digestion with two different restriction enzymes consistently showed that *FBXO32* was methylated in HeyC2 cells (Figure 2a). High-resolution bisulfite sequencing of 32 CpG sites showed that HeyC2 was densely methylated in this region. Approximately 30% of methylation was observed in IOSE cells, whereas the rest of the cells were essentially free of methylation (Figure 2b).

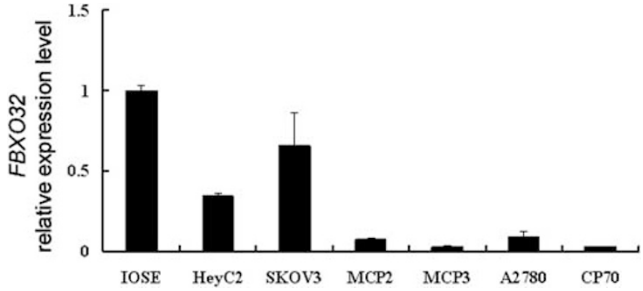

Figure 1 *FBXO32* expression in IOSE and ovarian cancer cell line. Total RNA was isolated from ovarian cells and converted into cDNA for amplification with specific primers for *FBXO32*. The relative level of expression after quantitative real-time RT-PCR was compared with IOSE (set as 100%). Each bar represents mean ± s.d.

Reexpression of *FBXO32* After Epigenetic Drug Treatment of Ovarian Cancer Cells

To quantify the methylation level of *FBXO32*, we designed a new set of primers for real-time qMSP assay on the basis of the previously described bisulfite sequencing. Consistent with the COBRA and bisulfite sequencing results, a significantly higher level methylation of *FBXO32* in HeyC2 cells compared with the other cancer (Figure 2c) or normal (Supplementary Figure S2) ovarian cells was observed using qMSP. Treatment with either the demethylating agent 5azaDC (Figure 3a) or HDAC inhibitor TSA (Figure 3b) lead to partial reexpression of *FBXO32* in all ovarian cancer cells and prominent *FBXO32* reactivation was observed in HeyC2, which had the highest level of *FBXO32* methylation. Interestingly, cells without *FBXO32* methylation (such as MCP2, MCP3, CP70, and A2780) showed higher levels of *FBXO32* reactivation after TSA treatment compared with 5azaDC. To exclude the possibility that high-dose 5azaDC treatment had additional effects (other than DNA demethylation) in the HeyC2 line, cells were treated with 0.5 μM of the DNMT inhibitor. Although the lower drug concentration had no obvious effect on reexpression of *FBXO32* (Supplementary Figure S3a), bisulfite sequencing showed that 0.5 μM of 5azaDC resulted in partial *FBXO32* demethylation as compared with complete demethylation at 5 μM of the treatment (Supplementary Figure S3b). Taken together, these results further show that *FBXO32* is silenced by promoter hypermethylation in HeyC2 cells and suggest that chromatin histone modifications, rather than DNA methylation, contribute to *FBXO32* gene silencing in MCP2, MCP3, CP70, and A2780 ovarian cancer cell lines.

Restoration of *FBXO32* Inhibits Growth of Ovarian Cancer Cells

Although a previous study showed that *FBXO32* is a tumor suppressor in breast cancer,[23] the role of *FBXO32* in ovarian

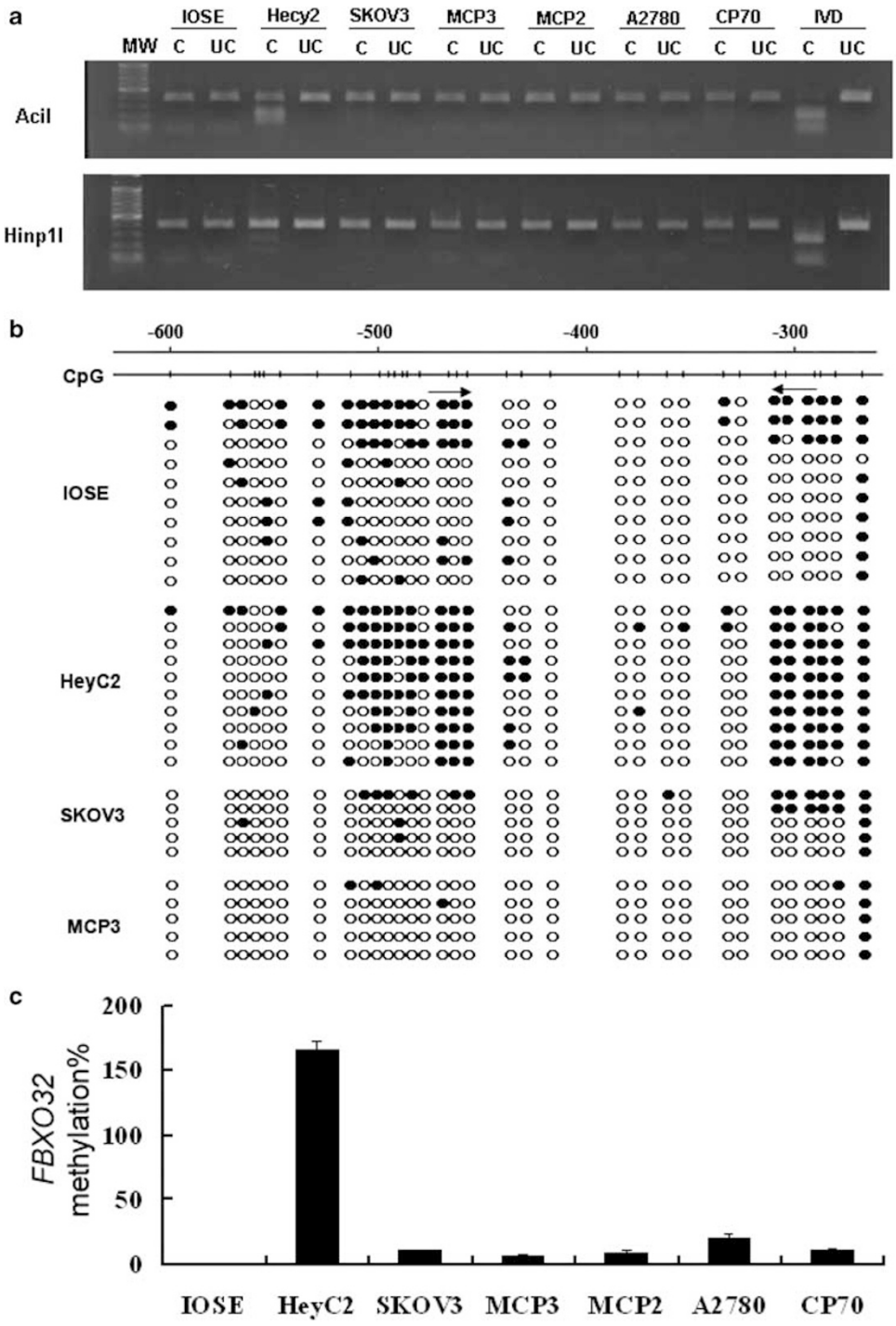

Figure 2 Methylation status of *FBXO32* in ovarian cell lines. (**a**) The methylation status of the *FBXO32* promoter region was analyzed by COBRA assay. Bisulfite-modified DNA was PCR amplified and digested with AciI and Hinp1I. C, digested by restriction enzyme; UC, undigested control. (**b**) Bisulfite sequencing analysis of the *FBXO32* promoter in four ovarian cell lines. Each vertical bar represents a CpG site in the promoter region, and the methylation status of the corresponding site is indicated in the circle below. Open and filled circles represent unmethylated and methylated CpG sites, respectively, and each row represents a single clone. The locations of the primers for subsequent methylation-specific PCR (MSP) reaction are also indicated by arrows. (**c**) Quantitative real-time MSP (qMSP) of *FBXO32* in ovarian cell lines. The DNA of ovarian cancer cell lines was bisulfite converted and the percentage of *FBXO32* methylation was determined by qMSP. The amount of methylated *FBXO32* was normalized by the amount of *ACTB* and expressed as the percentage of IVD (*in vitro* methylated DNA). Each bar represents mean ± s.d. of duplicate experiments.

cancer has not been investigated. To examine the effect of restoring *FBXO32* expression in ovarian cancer cells, cell proliferation MTS assays and colony-forming assays were performed. Transient transfection of two different vectors expressing *FBXO32* cDNA into CP70 (Figure 4a and b), Hey C2 (Figure 4d and e), and SKOV3 cells (Supplementary Figure S4) resulted in a reduction of size and number of colonies being formed. RT-PCR analysis confirmed the expression of *FBXO32* in these transient transfected cells (Figure 4c). Interestingly, transfection with the pcDNA3.1 vector showed a higher level of *FBXO32* expression corresponding to a >20-fold growth suppression as compared with the pIRES_EGFP, vector which showed a lower level of *FBXO32* expression and a 3-fold growth suppression (based on the number of colonies formed). Similar results were observed in *FBXO32* stable transfectants using MTS assays (Figure 5a and b).

Restoration of *FBXO32* Inhibits Tumor Growth *In Vivo*

To further examine the effect of *FBXO32* in CP70 cells *in vivo*, cells that were stably transfected with either *FBXO32* cDNA or control vector (pcDNA3.1) were injected subcutaneously into nude mice. Tumor growth from cells injected with control vector was first observed at day 9 after injection of CP70 cells (Figure 5c). From day 14 onward, there was a significant difference in tumor volume between cells transfected with *FBXO32* and control vector (D14: $0.05 \pm 0.037\,cm^3$ *vs* $0.174 \pm 0.056\,cm^3$, $P<0.005$; Supplementary Figure S5). Taken together, results from *in vitro* and *in vivo* indicate that *FBXO32* might be a tumor suppressor in ovarian cancer.

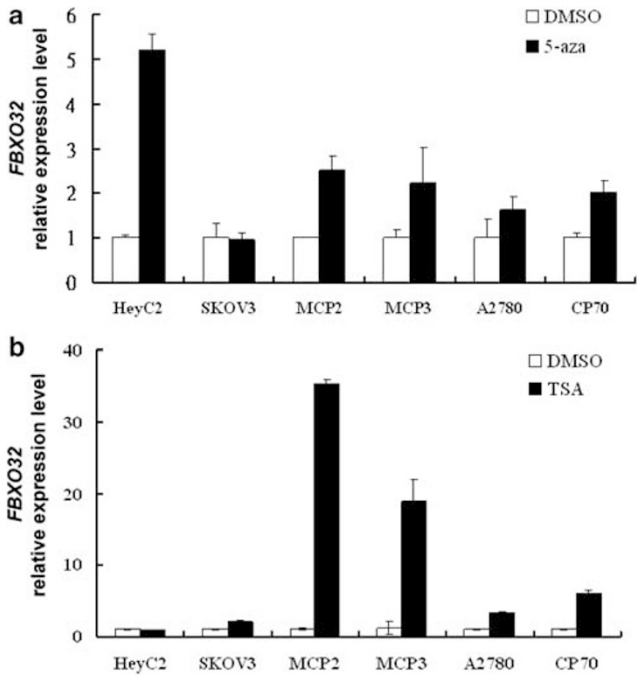

Figure 3 Expression level of *FBXO32* in ovarian cancer cell lines treated with 5-aza-2′-deoxycytidine (5azaDC) or trichostatin A (TSA). Ovarian cancer cells were either treated with (**a**) 0.5 μM 5-azaDC for 72 h or with (**b**) TSA for 12 h. The expression of *FBXO32* was determined by quantitative real-time RT-PCR and compared with the DMSO-treated control. Each bar represents mean ± s.d. of relative expression level of duplicate experiments.

FBXO32 Induces Apoptosis and Enhances Chemosensitivity to Cisplatin

Having shown that *FBXO32* inhibited the growth of ovarian cancer, it was of interest to examine the mechanism associated with this inhibition. As a previous study showed that *FBXO32* has a critical role in regulating apoptosis in breast cancer,[23] we investigated whether *FBXO32* induces apoptosis in ovarian cancer. Results from the FACS analysis showed that transfection of *FBXO32* enhanced apoptosis in CP70 cells as compared with vector control (apoptotic cell%, control: 2.55 ± 0.17; FBXO32: 10.72 ± 1.07, $P<0.05$; Figure 6a and b). We then investigated whether *FBXO32* can enhance the activity of a known apoptotic agent, cisplatin, in CP70 cells. As expected, CP70 showed chemoresistance to this agent (Figure 6b) as reported previously.[29] Interestingly, *FBXO32* markedly enhanced apoptosis of CP70 at the same dose of cisplatin (apoptotic cell%, control: 3.28 ± 0.24; FBXO32: 16.94 ± 0.25, $P<0.05$). Furthermore, MTS cytotoxicity assay showed that transfection of *FBXO32* induced an ~twofold increase in cisplatin sensitivity of CP70 cells (IC_{50}, control: 1.447 μg/ml; FBXO32-1: 0.892 μg/ml, and Figure 6c). Surprisingly, the same effect was not observed in HeyC2 cells, which have much higher drug resistance than do CP70 cells (IC_{50}, HeyC2: 5.6 μg/ml, CP70: 2.2 μg/ml, and Supplementary Figure S6). However, an increase in the G1 cell population was observed in *FBXO32*-transfected HeyC2 cells (Supplementary Table S2), suggesting that decreased cell-cycle progression may be responsible for the slower cell growth rate observed in those cells (Figure 5b).

FBXO32 Methylation Predicts Survival in Ovarian Cancer Patients

To investigate the clinical relevance of our *in vitro* findings, we used qMSP and immunohistochemistry to examine *FBXO32* methylation and expression in tumor samples ($n=96$) obtained from ovarian cancer patients (Supplementary Table S1). The median age at the time of diagnosis for this cohort was 52 years (range, 18–90 years). A total of 58 cases (60.4%) were at high stage (FIGO stage III and IV) and 38 cases (39.6%) were at low stage (FIGO stage I and II). A 30% methylation level was used as a cutoff to discriminate between clinicopathological parameters, on the basis of the level of methylation determined in NOSE cells. The methylation level of *FBXO32* was significantly associated with high-stage patients ($P=0.024$; Figure 7a and Table 1). No association between *FBXO32* methylation and age or grade was observed. On the other hand, samples with higher methylation had lower expression of FBXO32, although heterogeneous FBXO32 staining was observed (Supplementary Figure S7). Kaplan–Meier survival

curves showed that patients with high *FBXO32* methylation had significantly shorter PFS ($P = 0.027$) than patients with low *FBXO32* methylation (Figure 7b), indicating that *FBXO32* methylation may serve as a prognostic indicator. Although *FBXO32* methylation was not significantly associated with OS, the high methylation group tended to have shorter survival (Figure 7c, $P = 0.096$).

Interestingly, there was a group of patients displaying low *FBXO32* methylation (methylation $<15\%$) and also low OS (<36 months) (Supplementary Figure S8), indicating that

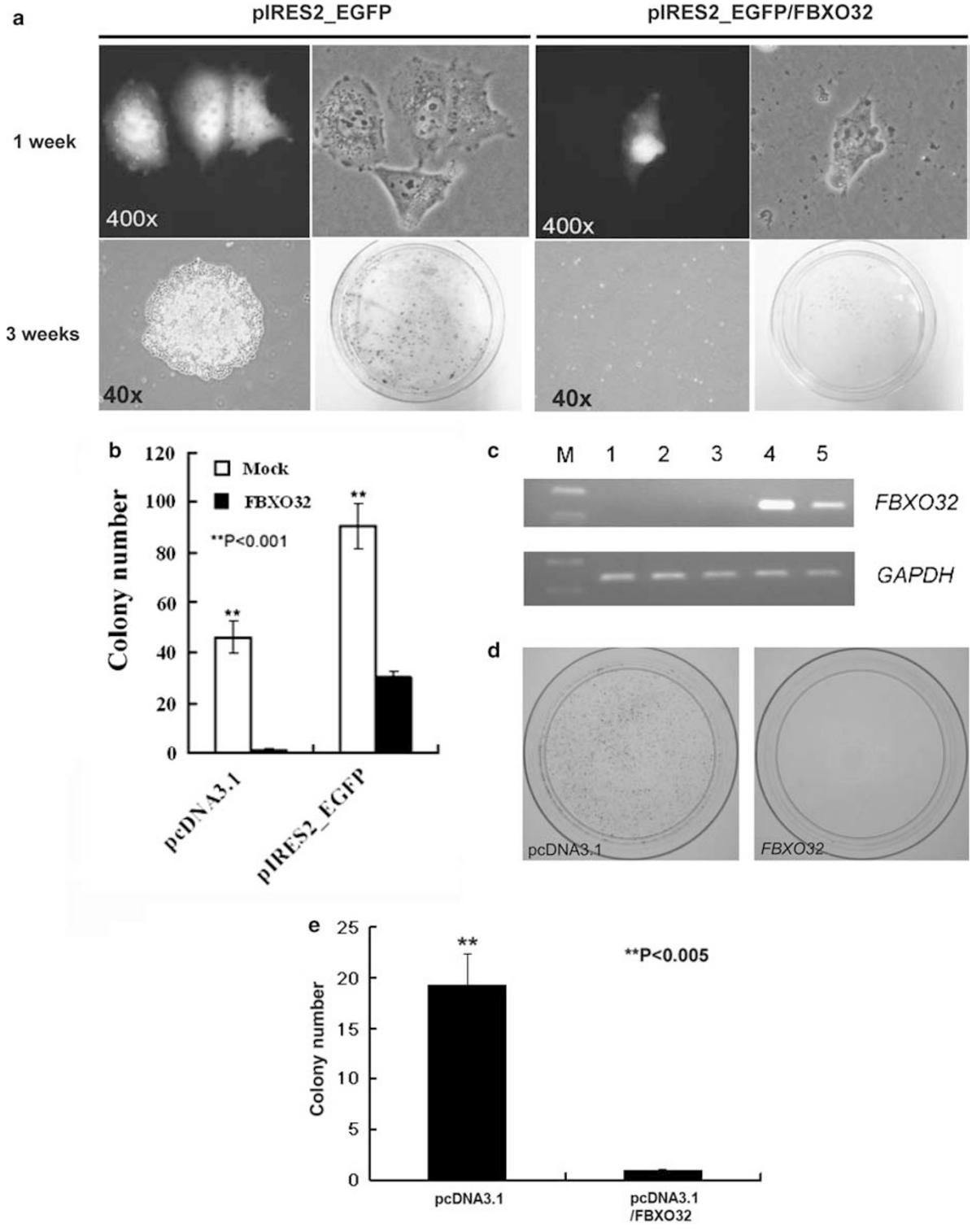

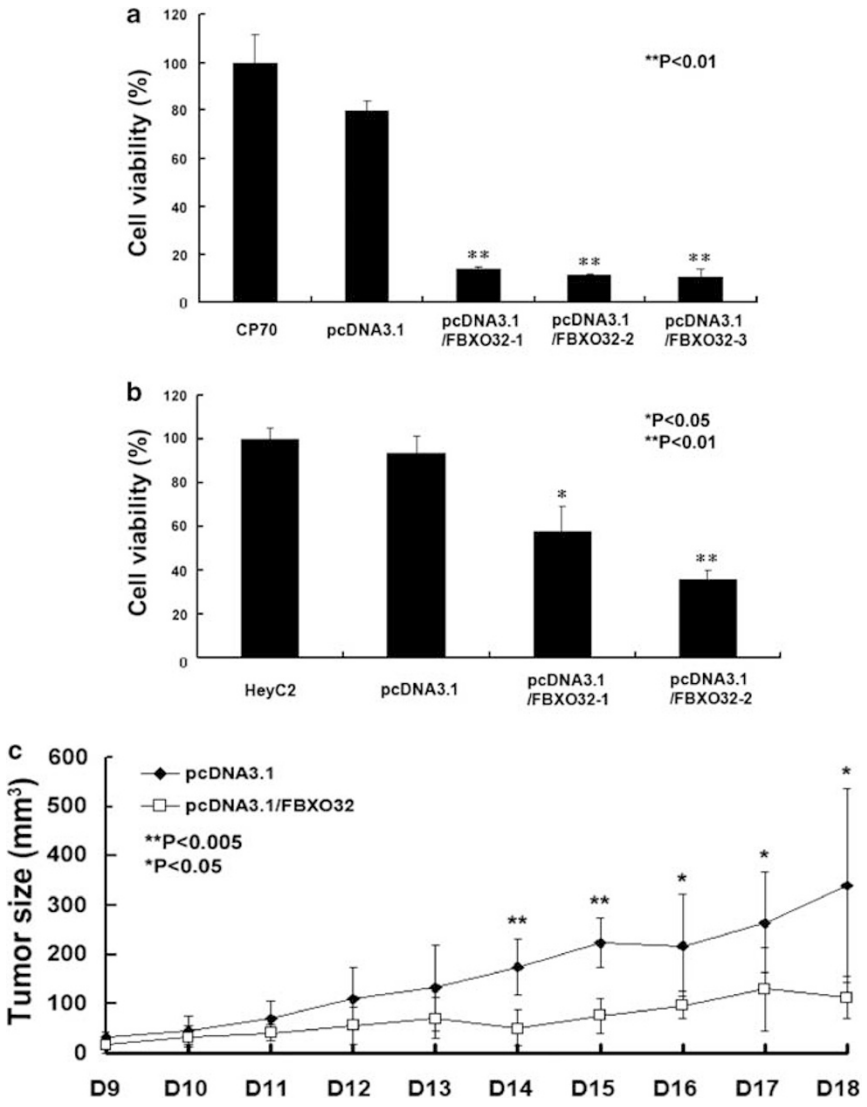

Figure 5 Effects of FBXO32 on growth of ovarian cancer cells. The effect of FBXO32 on the growth of CP70 (**a**) and HeyC2 (**b**) cells *in vitro* was determined by MTS assay. FBXO32 stable transfectants were seeded onto 96-well plates for 4 days. The number of cells at the end of the experiment was determined by colorimetric MTS assays. The results showed that restoration of *FBXO32* significantly inhibited the growth of CP70 and HeyC2 cells *in vitro*. (**c**) The effect of *FBXO32* on tumor growth *in vivo* was also determined by a nude mice model. CP70 cells stably transfected with FBXO32 or empty vector (pcDNA3.1) were injected subcutaneously into athymic nude mice. Tumor volumes were measured daily. From day 14 onward, the volume of tumors with *FBXO32* was significantly reduced compared with vector controls (**$P<0.005$, *$P<0.05$ and Supplementary Figure S5). Data were expressed as mean ± s.d. ($n=4$).

Figure 4 Effects of FBXO32 on the colony formation of ovarian cancer cells. (**a**) CP70 cells were transiently transfected with either pIRES2_EGFP (mock transfection, left) or plasmid expressing FBXO32 (pIRES2_EGFP/FBXO32, right). The fluorescence of EGFP was detected by fluorescence microscopy at the first week of the experiment (upper panel). FBXO32 transfectants showed significantly smaller and fewer colonies after G418 selection for 3 weeks (lower panel). (**b**) Quantitative analysis of the number of colonies formed by colony-forming assay. Cells transfected with either pcDNA3.1 or pIRES_EGFP expressing the FBXO32 vector showed a significant reduction in the number of colonies. The number of colonies formed using pcDNA3.1 (left) or pIRES2_EGFP (right) are mock *vs* *FBXO32*, 46.5 ± 6.36 *vs* 1.5 ± 0.7, $P<0.001$; 90.5 ± 9.19 *vs* 30.5 ± 2.12; $P<0.001$, respectively. (**c**) Expression analysis of *FBXO32* in CP70-transfected cells. In the upper panel, RT-PCR was performed to examine the expression status of *FBXO32* in CP70 cells transiently transfected with various plasmids. Lane 1: CP70 parental cells; lane 2: pcDNA 3.1; lane 3: pIRES2_EGFP; lane 4: pcDNA3.1/FBXO32, and lane 5: pIRES2_EGFP/FBXO32; M, 100-bp marker. Expression of *FBXO32* was only detected in cells transfected with *FBXO32* expression vector (lanes 4 and 5). Expression of *GAPDH* (lower panel) was also performed as internal control. (**d**) Similar experiment was performed in HeyC2 ovarian cancer cells. Transfection of *FBXO32* expression vector leads to significant reduction in the number of colonies in HeyC2 cells. (**e**) Quantitative analysis of colony-forming assay showed that the number of colonies formed were greater ($P<0.005$) in mock *vs* FBXO32 (19.33 ± 3.06 *vs* 1 ± 0). The color reproduction of this figure is available on the html full text version of the manuscript.

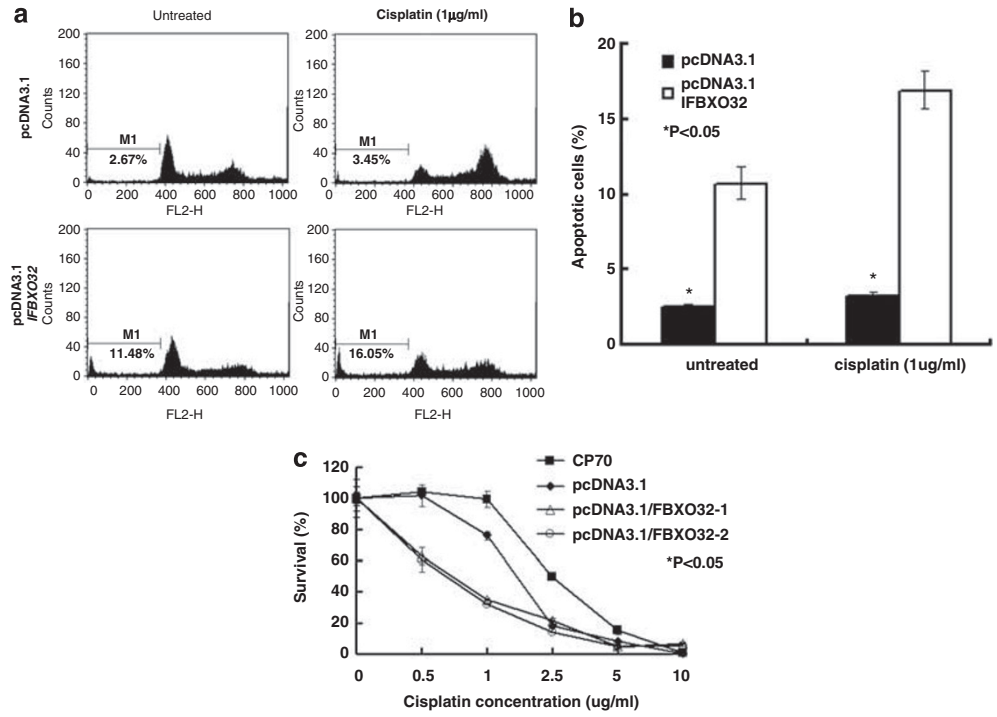

Figure 6 Effect of FBXO32 on apoptosis and chemosensitivity of CP70 ovarian cancer cells. Cells were treated with or without cisplatin (1 μg/ml) for 24 h. DNA fragmentation was measured by FACS analysis. (**a**) DNA fluorescence histogram of propidium iodide-stained cells. FBXO32 enhances apoptosis in CP70 cells as determined by the sub-G1 area (marked by M1 in the histogram). This effect is more prominent in cells treated with cisplatin. (**b**) Percentage of apoptotic cells in the sub-G1 area. Data are expressed as mean ± s.d. ($n = 3$) (*$P < 0.05$). (**c**) The effect of FBXO32 on chemosensitivity of CP70 to cisplatin was also determined by MTS cytotoxicity assay. Cells seeded on a 96-well plate were treated with various concentrations of cisplatin for 4 days. At the end of the experiment, cell numbers (expressed as survival%) were determined by colorimetric MTS assay. The mean ± s.d. on each concentration of cisplatin were shown (*$P < 0.05$).

tumorigenesis in this group of patients may be independent of *FBXO32* methylation. Exclusion of this extreme group from the analysis resulted in a significant association of *FBXO32* methylation with stage ($P = 0.007$), and marginally with grade ($P = 0.052$; Table 1).

As the above-mentioned approaches used a cutoff value and may have biased the data analysis, a multivariate analysis was performed to analyze *FBXO32* methylation (on a continuous scale) and age for their predictive values on OS and PFS. The results from Cox proportional hazards model are shown in Table 2. *FBXO32* methylation was predictive of PFS (hazard ratio: 1.003, $P = 0.028$) but not OS ($P = 0.095$). As expected, age was also a significant prognostic factor for OS ($P = 0.011$). Exclusion of the extreme group also resulted in a significant association of *FBXO32* methylation with PFS ($P = 0.008$) and OS ($P = 0.008$), which is similar to the Kaplan–Meier analysis showing that high *FBXO32* methylation levels are associated with shorter survival.

DISCUSSION

Dysregulation of TGF-β signaling pathway is a common event in ovarian cancer and crucial for ovarian cancer carcinogenesis.[4] Recent studies have further shown that disruption of an upstream signaling pathway regulator may result in transcriptional repression of a downstream target gene through epigenetic mechanisms,[15,30] and our previous study showed that dysregulation of TGF-β/SMAD4 signaling lead to epigenetic silencing of its downstream target, *ADAM19* in ovarian cancer cells with impaired SMAD4 nuclear translocation.[15]

In this study, our investigation of another TGF-β/SMAD4 downstream target, *FBXO32*, further supports this hypothesis. We found that *FBXO32* is expressed in normal OSE cells but downregulated in ovarian cancer cells. Although this downregulation was mediated through DNA methylation in HeyC2 cells showing constitutive SMAD4 nuclear translocation[15] (Supplementary Figure S9), downregulation of *FBXO32* in ovarian cancer cells with impaired SMAD4 nuclear translocation (MCP2, MCP3, A2780, and CP70) was independent of DNA methylation.[15] Methylation of *FBXO32* in HeyC2 cells may be due to long-term, constitutive activation of SMAD4; however, the role of SMAD4 in the methylation of *FBXO32* warrants further investigation. Furthermore, we observed the downregulation of another TGF-β/SMAD4 target, *RunX1T1*, by promoter hypermethylation in HeyC2 cells (data not shown). Although our studies on the role of TGF-β in *RUNX1T1* hypermethylation are currently ongoing, this result suggests that dysregulation of

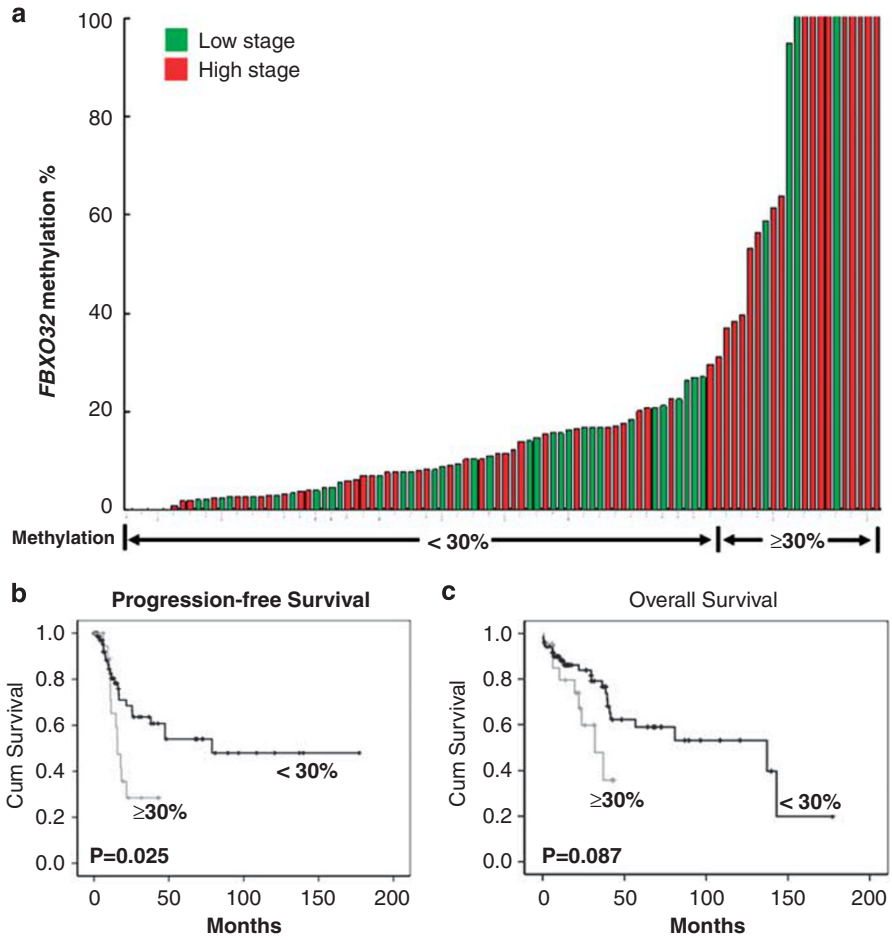

Figure 7 Association between methylation level of *FBXO32* and survival in 96 ovarian cancer patient samples. (**a**) Histogram showing the methylation level of *FBXO32* in 96 ovarian cancer samples detected by qMSP. Samples with methylation level $\geq 30\%$ were considered as methylated and were indicated. The red and green bars indicate samples of high- and low-stage tumor, respectively. It is interesting to note that most of the methylated samples are of high-stage tumor ($P < 0.05$, Table 1). Kaplan–Meier analysis for progression-free survival (**b**) and overall survival (**c**) in 96 ovarian cancer samples is shown. Patients were grouped according to the *FBXO32* methylation level of 30%, which is based on the methylation level of NOSE cells. Patients with high *FBXO32* methylation have significant shorter progression-free survival. Log-rank *P*-values are shown.

the TGF-β signaling pathway may contribute to concurrent methylation of tumor-suppressor genes in cancer, a phenomenon known as CpG island methylator phenotype, CIMP.[31] In contrast, silencing of *FBXO32* in ovarian cancer cells with impaired SMAD4 nuclear translocation seems to be mediated by chromatin histone changes (Figure 3b), as we have observed for another TGF-β downstream target, *ADAM19*.[15] In support of this possibility, a previous study reported that inhibition of the polycomb-repressive complex 2 by DZNep restored expression of *FBXO32* in MCF7 cells. We observed that treatment with TSA, which has been shown to remove repressive histone marks, restored *FBXO32* expression in cells without *FBXO32* methylation (MCP2, MCP3, A2780, and CP70). In contrast, treatment with the DNMT inhibitor 5azaDC did not result in the reexpression of *FBXO32* in MCF7 cells, although partial demethylation was observed.[23] This discrepancy may be attributed to the fact that low-dose 5azaDC (0.5 μM) leads to only partial demethylation of *FBXO32*, whereas complete demethylation is required for the reactivation of this gene (Supplementary Figure S3). However, it is possible that the mechanism of *FBXO32* silencing in breast cancer cells may be different than in ovarian cancer, and off-target effects of 5azaDC cannot be overlooked. In support of this latter possibility, inhibition of G9a histone methyltransferase decreased histone H3K9 dimethylation,[32] and 5azaDC can upregulate genes without causing detectable demethylation,[33,34] perhaps explaining the partial reactivation of *FBXO32* by 0.5 μM of 5azaDC in MCP2 and MCP3 cells (data not shown).

FBXO32 belongs to the F-box protein family of the SCF ubiquitin protein ligase complex involved in muscle atrophy.[22] However, a previous study showed that the AKT signaling pathway negatively regulates *FBXO32*,[24] thus implying that it may also be involved in regulating cell survival.[23] More

Table 1 Association between methylation of *FBXO32* and clinicopathological features of 96 ovarian cancer patients

	All cases		Extreme cases removed	
	Methylation %	*P*-value	Methylation %	*P*-value
Age (years)				
≧60	22.6 (7/31)		35.0 (7/20)	
<60	21.5 (14/65)	0.552	35.8 (14/39)	0.590
Stage[a]				
High	29.3 (17/58)		50.0 (17/34)	
Low	10.5 (4/38)	**0.024**[c]	16.0 (4/25)	**0.007**
Grade[b]				
High	25.0 (19/76)		42.2 (19/45)	
Low	10.5 (2/19)	0.146	14.3 (2/14)	0.052

Mean ± s.d.

Extreme cases are excluded from analysis (see the 'MATERIAL AND METHODS' section).

[a]High and low stage are defined as FIGO stage III and IV and stage I and II, respectively.

[b]High and low grade are defined as grade 2–3 and 1, respectively. Grade information was not available for one patient.

[c]Bold value indicates $P<0.05$.

Table 2 Multivariate analysis of survival by Cox proportional hazards model

Variable	Overall survival		Progression-free survival	
	HR (95% CI)	*P*-value	HR (95% CI)	*P*-value
FBXO32 methylation	1.002 (1.000–1.005)	0.095	1.003 (1.000–1.006)	**0.028**
Age	1.034 (1.008–1.062)	**0.011**[b]	1.018 (0.994–1.042)	0.137
FBXO32 methylation[a]	1.004 (1.001–1.008)	**0.008**	1.004 (1.001–1.007)	**0.008**
Age[a]	1.029 (0.997–1.061)	0.073	1.016 (0.989–1.044)	0.256

[a]Extreme cases were excluded from analysis (see the 'MATERIAL AND METHODS' section).

[c]Bold value indicates $P<0.05$.

recently, *FBXO32* has been shown to be upregulated by tumor necrosis factor, a signaling which is known to be involved in regulating apoptosis.[35] In this study, we found that restoration of *FBXO32* reduced tumor growth *in vitro* and *in vivo*, perhaps because of increased cellular apoptosis. To further investigate this possibility, we restored *FBXO32* expression in drug-resistant ovarian cancer cells and examined the ability of cisplatin to induce apoptosis. Interestingly, *FBXO32* resensitized CP70 cells to cisplatin and markedly enhanced apoptosis. On the contrary, *FBXO32* reexpression only caused a decrease in cell-cycle progression in HeyC2 cells, which have a much higher drug resistance than do CP70 cells, suggesting that the mechanism of *FBXO32*-mediated growth suppression differs in the two ovarian cancer cell lines. Together with recent findings that two other members of F-Box protein FBXW7 and FBX4 can function as tumor suppressors,[36,37] FBXO32 may be a novel tumor suppressor in ovarian cancer, and downregulation of *FBXO32* may impair TGF-β-mediated growth inhibition in ovarian cancer as observed in our previous study.[15]

To explore the relationship between clinicopathological features and methylation of *FBXO32*, we performed qMSP on ovarian carcinomas. A high level of *FBXO32* methylation was significantly associated with higher stage and shorter PFS, thus suggesting that silencing of *FBXO32* may be crucial to ovarian cancer progression and may have the potential to serve as a new prognostic marker for the disease. It is important to note that a group of patients displayed low *FBXO32* methylation and low OS. Excluding that group from the analysis resulted in a further significant association between stage, grade, and survival (both OS and PFS). It is unclear why the survival of this group of patients was independent of *FBXO32* methylation, but one possibility could be that the TGF-β signaling pathway was disrupted in those tumors, as we have observed in ovarian cancer cell lines (impaired SMAD4 nuclear translocation was seen in MCP3, MCP2, A2780, and CP70 cell lines[15]; Figure 2).

In conclusion, we show that *FBXO32* is epigenetically silenced in ovarian cancer cells with impaired TGF-β/SMAD4 signaling and may be a novel tumor suppressor in ovarian cancer. As a high level of *FBXO32* methylation predicts survival in ovarian cancer patients, we suggest that *FBXO32* may serve as a methylation biomarker for the disease.

Supplementary Information accompanies the paper on the Laboratory Investigation website (http://www.laboratoryinvestigation.org)

ACKNOWLEDGEMENTS

We thank Drs Yeu-Wei Leu and Hau-Ren Chen for their technical assistance. This study was supported by research grant from National Science Council, Republic of China: NSC97-2320-B-194-002-MY3, NSC96-2314-B-194-002 and National Health Research Institute, Republic of China: NHRI-EX98-9717NC.

DISCLOSURE/CONFLICT OF INTEREST

The authors declare no conflict of interest.

1. Wakabayashi MT, Lin PS, Hakim AA. The role of cytoreductive/debulking surgery in ovarian cancer. J Natl Compr Canc Netw 2008;6:803–810; quiz 811.
2. Sogaard M, Kjaer SK, Gayther S. Ovarian cancer and genetic susceptibility in relation to the BRCA1 and BRCA2 genes. Occurrence, clinical importance and intervention. Acta Obstet Gynecol Scand 2006;85:93–105.
3. Nossov V, Amneus M, Su F, *et al.* The early detection of ovarian cancer: from traditional methods to proteomics. Can we really do better than serum CA-125? Am J Obstet Gynecol 2008;199:215–223.

4. Nilsson EE, Skinner MK. Role of transforming growth factor beta in ovarian surface epithelium biology and ovarian cancer. Reprod Biomed Online 2002;5:254–258.
5. Wong AS, Leung PC. Role of endocrine and growth factors on the ovarian surface epithelium. J Obstet Gynaecol Res 2007;33:3–16.
6. Yamada SD, Baldwin RL, Karlan BY. Ovarian carcinoma cell cultures are resistant to TGF-beta1-mediated growth inhibition despite expression of functional receptors. Gynecol Oncol 1999;75:72–77.
7. Hu W, Wu W, Nash MA, *et al.* Anomalies of the TGF-beta postreceptor signaling pathway in ovarian cancer cell lines. Anticancer Res 2000;20:729–733.
8. Balch C, Fang F, Matei DE, *et al.* Minireview: epigenetic changes in ovarian cancer. Endocrinology 2009;150:4003–4011.
9. Simon JA, Lange CA. Roles of the EZH2 histone methyltransferase in cancer epigenetics. Mutat Res 2008;647:21–29.
10. Mulero-Navarro S, Esteller M. Epigenetic biomarkers for human cancer: the time is now. Crit Rev Oncol Hematol 2008;68:1–11.
11. McKenna ES, Roberts CW. Epigenetics and cancer without genomic instability. Cell Cycle 2009;8:23–26.
12. Caslini C, Capo-chichi CD, Roland IH, *et al.* Histone modifications silence the GATA transcription factor genes in ovarian cancer. Oncogene 2006;25:5446–5461.
13. Yu Y, Fujii S, Yuan J, *et al.* Epigenetic regulation of ARHI in breast and ovarian cancer cells. Ann NY Acad Sci 2003;983:268–277.
14. Chan MW, Wei SH, Wen P, *et al.* Hypermethylation of 18S and 28S ribosomal DNAs predicts progression-free survival in patients with ovarian cancer. Clin Cancer Res 2005;11:7376–7383.
15. Chan MW, Huang YW, Hartman-Frey C, *et al.* Aberrant transforming growth factor beta1 signaling and SMAD4 nuclear translocation confer epigenetic repression of ADAM19 in ovarian cancer. Neoplasia 2008;10:908–919.
16. Su HY, Lai HC, Lin YW, *et al.* An epigenetic marker panel for screening and prognostic prediction of ovarian cancer. Int J Cancer 2009;124:387–393.
17. Wei SH, Chen CM, Strathdee G, *et al.* Methylation microarray analysis of late-stage ovarian carcinomas distinguishes progression-free survival in patients and identifies candidate epigenetic markers. Clin Cancer Res 2002;8:2246–2252.
18. Wei SH, Balch C, Paik HH, *et al.* Prognostic DNA methylation biomarkers in ovarian cancer. Clin Cancer Res 2006;12:2788–2794.
19. Qin H, Chan MW, Liyanarachchi S, *et al.* An integrative ChIP-chip and gene expression profiling to model SMAD regulatory modules. BMC Syst Biol 2009;3:73.
20. Bodine SC, Latres E, Baumhueter S, *et al.* Identification of ubiquitin ligases required for skeletal muscle atrophy. Science 2001;294: 1704–1708.
21. Li HH, Kedar V, Zhang C, *et al.* Atrogin-1/muscle atrophy F-box inhibits calcineurin-dependent cardiac hypertrophy by participating in an SCF ubiquitin ligase complex. J Clin Invest 2004;114:1058–1071.
22. Hanai J, Cao P, Tanksale P, *et al.* The muscle-specific ubiquitin ligase atrogin-1/MAFbx mediates statin-induced muscle toxicity. J Clin Invest 2007;117:3940–3951.
23. Tan J, Yang X, Zhuang L, *et al.* Pharmacologic disruption of polycomb-repressive complex 2-mediated gene repression selectively induces apoptosis in cancer cells. Genes Dev 2007;21:1050–1063.
24. Stitt TN, Drujan D, Clarke BA, *et al.* The IGF-1/PI3K/Akt pathway prevents expression of muscle atrophy-induced ubiquitin ligases by inhibiting FOXO transcription factors. Mol Cell 2004;14:395–403.
25. Ahluwalia A, Hurteau JA, Bigsby RM, *et al.* DNA methylation in ovarian cancer. II. Expression of DNA methyltransferases in ovarian cancer cell lines and normal ovarian epithelial cells. Gynecol Oncol 2001;82: 299–304.
26. Gillan L, Matei D, Fishman DA, *et al.* Periostin secreted by epithelial ovarian carcinoma is a ligand for alpha(V)beta(3) and alpha(V)beta(5) integrins and promotes cell motility. Cancer Res 2002;62:5358–5364.
27. Chan MW, Chu ES, To KF, *et al.* Quantitative detection of methylated SOCS-1, a tumor suppressor gene, by a modified protocol of quantitative real time methylation-specific PCR using SYBR green and its use in early gastric cancer detection. Biotechnol Lett 2004;26:1289–1293.
28. Cheng AS, Jin VX, Fan M, *et al.* Combinatorial analysis of transcription factor partners reveals recruitment of c-MYC to estrogen receptor-alpha responsive promoters. Mol Cell 2006;21:393–404.
29. Henkels KM, Turchi JJ. Induction of apoptosis in cisplatin-sensitive and -resistant human ovarian cancer cell lines. Cancer Res 1997;57: 4488–4492.
30. Bagnyukova TV, Tryndyak VP, Muskhelishvili L, *et al.* Epigenetic downregulation of the suppressor of cytokine signaling 1 (Socs1) gene is associated with the STAT3 activation and development of hepatocellular carcinoma induced by methyl-deficiency in rats. Cell Cycle 2008;7:3202–3210.
31. Issa JP. CpG island methylator phenotype in cancer. Nat Rev Cancer 2004;4:988–993.
32. Tachibana M, Sugimoto K, Fukushima T, *et al.* Set domain-containing protein, G9a, is a novel lysine-preferring mammalian histone methyltransferase with hyperactivity and specific selectivity to lysines 9 and 27 of histone H3. J Biol Chem 2001;276:25309–25317.
33. Wozniak RJ, Klimecki WT, Lau SS, *et al.* 5-Aza-2′-deoxycytidine-mediated reductions in G9A histone methyltransferase and histone H3 K9 di-methylation levels are linked to tumor suppressor gene reactivation. Oncogene 2007;26:77–90.
34. Guilleret I, Benhattar J. Demethylation of the human telomerase catalytic subunit (hTERT) gene promoter reduced hTERT expression and telomerase activity and shortened telomeres. Exp Cell Res 2003;289:326–334.
35. Moylan JS, Smith JD, Chambers MA, *et al.* TNF induction of atrogin-1/MAFbx mRNA depends on Foxo4 expression but not AKT-Foxo1/3 signaling. Am J Physiol Cell Physiol 2008;295:C986–C993.
36. Lin DI, Barbash O, Kumar KG, *et al.* Phosphorylation-dependent ubiquitination of cyclin D1 by the SCF(FBX4-alphaB crystallin) complex. Mol Cell 2006;24:355–366.
37. Fujii Y, Yada M, Nishiyama M, *et al.* Fbxw7 contributes to tumor suppression by targeting multiple proteins for ubiquitin-dependent degradation. Cancer Sci 2006;97:729–736.